

Field distributions in heavy mesons and baryons

D.S.Kuzmenko* Yu.A.Simonov †

*Institute of Theoretical and Experimental Physics,
117218, Moscow, Russia*

Abstract

Field distributions generated by static $Q\bar{Q}$ and QQQ sources are calculated analytically in the framework of the Field Correlator Method (FCM) using Gaussian (bilocal) correlator. In both cases the string consists mostly of longitudinal color electric field, while transverse electric field contributes locally less than 3%, in agreement with earlier lattice studies. In the QQQ case the profile of the Y shape was calculated for the first time and found to have a complicated structure with a deep hole at the string junction position. Possible consequences of this form for the baryon structure are discussed.

1. Field distributions inside the string connecting static $Q\bar{Q}$ sources have been measured repeatedly on the lattice using both connected [1, 2] and disconnected [3, 4] probes. Similar measurements were done later also for Abelian projected configurations [5]. Analytic calculations for the disconnected probe made in [6, 7] in the framework of the Gaussian approximation to the FCM [8, 9] have revealed a clear string-like structure of the same type as was found on the lattice.

However the connected probe yields an independent and more direct information on the field distribution in the string, which agrees with that of disconnected probe in general features of the action profile, however yields in addition particular details on the longitudinal and transverse components.

A detailed comparison of lattice data [1] with analytic predictions of FCM was done in [2], demonstrating a remarkable agreement in all distributions. In particular, the measured decrease of longitudinal electric field E_{\parallel} with distance from the string axis ("the string profile") agrees remarkably well with contribution of the lowest, (bilocal) correlator [2]. It should be noted that the input of FCM is the form of the field correlator, which is taken from the lattice measurements [12], yielding an exponential form of both scalar formfactors D and D_1 [8] with the slope $T_g \approx 0.2\text{fm}$. The dominance of the bilocal correlator (sometimes called the Gaussian Stochastic Model (GSM) of the QCD vacuum) was proved recently on the lattice by the precision measurement of Wilson loops (static potential) in different $SU(3)$ representations [10]. Analysis of data [10] made in [11] has confirmed that GSM contributes around 99% to the static $Q\bar{Q}$ potential.

*e-mail: kuzmenko@heron.itep.ru

†e-mail: simonov@heron.itep.ru

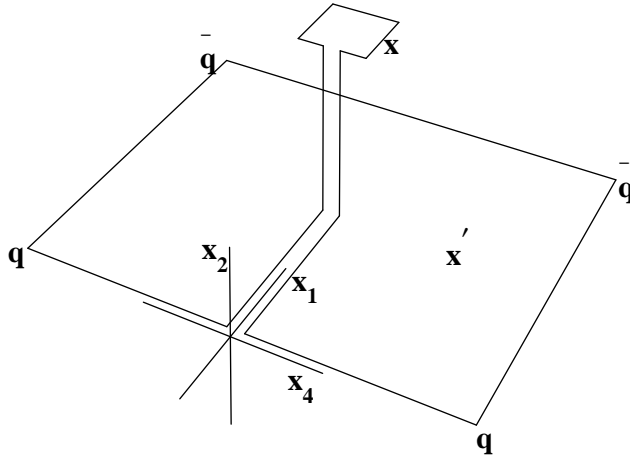


Figure 1: The connected probe in $Q\bar{Q}$ case.

These results give an additional stimulus to the analytic calculation of field distributions using lowest bilocal correlator. Our purpose in this letter is to calculate 3d field distributions to demonstrate the string formation, and in particular to study transverse electric fields and nonconfining piece (D_1) of the bilocal correlator which was not done in [2]. In addition we calculate for the first time the field distributions in the static QQQ system as a function of distance between quarks forming an equilateral triangle.

It will be shown that for the lowest energy configuration (the so-called Y - shaped, or string-junction configuration) the field distribution has a rather peculiar form with a hole at the place of the string-junction. The analysis of equations reveals the reason of this shape, and yields an estimate of the size and depth of the hole.

The plan of the paper is as follows. In section 2 necessary formulas are derived in the framework of FCM for the connected-probe field distributions. The $Q\bar{Q}$ case is treated in detail and 3d distributions are given. In section 3 the QQQ case is considered and the relief of the Y - shaped string is given. The hole at the center is demonstrated analytically and its parameters are found. In section 4 the $3Q$ potential is derived and compared with lattice measurements. In conclusion possible physical consequences and relation to the real case of heavy and light hadrons are discussed.

2. We follow in this section notations and methods used previously in [2]. The connected probe $\rho_{\mu\nu}(x)$ is made with the infinitesimal plaquette $P_{\mu\nu}$ at the point x , connected by parallel transporters (Schwinger lines) L, L^+ to the contour C of the Wilson loop W as shown in Fig.1.

$$\rho_{\mu\nu}(x) = \frac{\langle \text{tr}(WLP_{\mu\nu}(x)L^+) \rangle}{\langle \text{tr}W \rangle} - 1 \equiv \langle P_{\mu\nu}(x) \rangle_{Q\bar{Q}}. \quad (1)$$

In the continuum limit the size a of the plaquette $P_{\mu\nu}$ tends to zero and one has

$$\langle P_{\mu\nu}(x) \rangle_{Q\bar{Q}} \rightarrow a^2 \langle F_{\mu\nu}(x) \rangle_{Q\bar{Q}}. \quad (2)$$

To calculate (1) one can use the cluster expansion theorem [8] applied to the complex Wilson loop \bar{C} consisting of the original contour C and the plaquette $P_{\mu\nu}$ attached with the lines L, L^+ . In the Gaussian (bilocal) approximation one can proceed as in [2] to obtain the

final result for the contribution of the lowest correlator, $\langle FF \rangle$,

$$\rho_{\mu\nu}(x) = a^2 \int_{S(C)} d\sigma_{\rho\lambda}(x') D_{\rho\lambda,\mu\nu}(x', x) + O(a^4). \quad (3)$$

Here $S(C)$ is the minimal area surface inside the contour C , and D is

$$D_{\rho\lambda,\mu\nu}(x', x) = \frac{g^2}{N_c} \text{tr} \langle F_{\rho\lambda}(x') \Phi(x', x) F_{\mu\nu}(x) \Phi(x, x') \rangle, \quad (4)$$

while $\Phi(x, y)$ is parallel transporter, connecting points x, y . For the gauge-invariant function $D_{\rho\lambda,\mu\nu}$ there exist an expression in terms of two scalar functions D and D_1 (see second ref. in [8]),

$$\begin{aligned} D_{\rho\lambda,\mu\nu}(x, y) &= (\delta_{\rho\mu}\delta_{\lambda\nu} - \delta_{\rho\nu}\delta_{\mu\lambda})D(h) + \\ &\frac{1}{2} \left[\frac{\partial}{\partial h_\rho} h_\mu \delta_{\lambda\nu} - \frac{\partial}{\partial h_\lambda} h_\mu \delta_{\rho\nu} + \rho\lambda \leftrightarrow \mu\nu \right] D_1(h), \end{aligned} \quad (5)$$

where $h \equiv x - y$. The functions D, D_1 have been measured on the lattice [12] and were found to be exponential beyond $x = 0.2$ fm.

Here we use the exponential ansatz in the whole region of x , as it was done previously in [2], with parameters as in [12],[2]

$$D(x) = D(0) \exp(-\mu|x|), \quad D_1(x) = D_1(0) \exp(-\mu|x|), \quad (6)$$

$$D_1(0) \approx \frac{1}{3}D(0), \quad \mu \approx 1 \text{GeV}.$$

In the same Gaussian approximation, i.e. neglecting all higher correlators (which is accurate to better than one percent for static potentials [10, 11]) $D(0)$ can be expressed through the string tension

$$\sigma = \frac{1}{2} \int D(x) d^2x = \pi D(0)/\mu^2. \quad (7)$$

This connection will be important in what follows for the correct normalization of the field distribution in $Q\bar{Q}$ and QQQ .

The axes are shown in Fig.1. Contour C of Wilson loop is rectangular $C = R \times T$ and lies in the plane (14). It has coordinates $x' = (x'_1, x'_2, x'_3, x'_4)$: $0 \leq x'_1 \leq R, x'_2 = x'_3 = 0, -T/2 \leq x'_4 \leq T/2$. The probe is at $x = (x_1, x_2, x_3, x_4)$. x_1 is coordinate of probe along string axis, x_2 is distance of probe to the string axis; $x_3 = x_4 = 0$. The only nonzero components of color field are electric ones in x_1 and x_2 directions (see [2] for symmetry arguments and discussion). The resulting equations are directly obtained from (2-5) ($\rho_{i4}(x_1, x_2) = a^2 \langle E_i(x_1, x_2) \rangle_{Q\bar{Q}} \equiv a^2 E_i(x_1, x_2)$):

$$E_1(x_1, x_2) = \int_0^R dx'_1 \int_{-\frac{T}{2}}^{\frac{T}{2}} dx'_4 [D(0) + D_1(0) - \mu \frac{h_4^2 + h_1^2}{2h} D_1(0)] e^{-\mu h}, \quad (8)$$

$$E_2(x_1, x_2) = -\mu x_2 \int_0^R dx'_1 \int_{-\frac{T}{2}}^{\frac{T}{2}} dx'_4 \frac{(x_1 - x'_1)}{2h} D_1(0) e^{-\mu h}. \quad (9)$$

Here we have defined

$$h_4 = -x'_4, \quad h_1 = x_1 - x'_1; \quad h^2 = h_4^2 + h_1^2 + x_2^2. \quad (10)$$

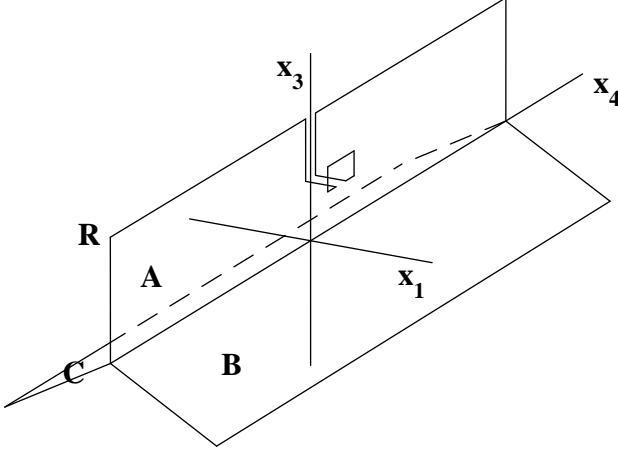


Figure 5: The connected probe in QQQ case.

The field distributions $E_1^2(x_1, x_2)$ are shown in Fig.2 (a-c) for different quark separations, $R = T_g, 5T_g$ and $15T_g$. The string profile, i.e. $E_1^2(x_2)$ distribution in the middle of the string, for these quark separations is shown in Fig.2 (d). One can see a clear string-like formation with the width of $2.2T_g$. The value of E_1 in the middle of string does not depend on R for R greater than $5T_g$. The saturated value is $E^{sat} = 1.8\text{GeV/fm}$.

The field distribution $E_2(x_1, x_2)$ is shown in Fig.3 for $R = 15T_g$. Note that $|E_2|$ is much smaller than $|E_1|$, $\max(|E_2(x_1, x_2)|) \sim 3\% \max(|E_1(x_1, x_2)|)$.

In Fig.4 a separate distribution $E_1(x_1, x_2)$ is shown generated by $D_1(x)$. One can see that D_1 does not produce a string, which is in agreement with the fact, that D_1 does not contribute to the string tension (7).

3. In case of the QQQ system the contour C consists of three contours connected by the string-junction trajectory, as depicted in Fig.5. The surface S consists of three surfaces Σ_A, Σ_B and Σ_C , and the probing plaquette $P_{\mu\nu}$ is attached by Schwinger lines L, L^+ to one of the static quark trajectories.

Choosing the axes as shown in Fig.5, $x_2 = 0$, one has two main contributing correlators $D_{14,14}$ and $D_{34,34}$ and a subleading nondiagonal one $D_{14,34} = D_{34,14}$. As a result one obtains the following field distributions (choosing $x_4 = 0$ for the plaquette $P_{\mu\nu}$ as in the $Q\bar{Q}$ case):

$$E_1^{(3Q)}(x_1, x_3) = \int (d\sigma_A \Lambda_{14}^{(A)} + d\sigma_B \Lambda_{14}^{(B)} + d\sigma_C \Lambda_{14}^{(C)}), \quad (11)$$

$$E_3^{(3Q)}(x_1, x_3) = \int (d\sigma_A \Lambda_{34}^{(A)} + d\sigma_B \Lambda_{34}^{(B)} + d\sigma_C \Lambda_{34}^{(C)}), \quad (12)$$

where we have defined

$$d\sigma_A \Lambda_{14}^{(A)} = dx'_4 dx'_3 D_{34,14}(x - x'), \quad (13)$$

$$d\sigma_B \Lambda_{14}^{(B)} = \frac{\sqrt{3}}{2} dx'_4 dl' D_{14,14} - \frac{1}{2} dx'_4 dl' D_{34,14}, \quad (14)$$

$$d\sigma_C \Lambda_{14}^{(C)} = -\frac{\sqrt{3}}{2} dx'_4 dl' D_{14,14} - \frac{1}{2} dx'_4 dl' D_{34,14}, \quad (15)$$

$$d\sigma_A \Lambda_{34}^{(A)} = dx'_4 dx'_3 D_{34,34}(x - x'), \quad (16)$$

$$d\sigma_B \Lambda_{34}^{(B)} = \frac{\sqrt{3}}{2} dx'_4 dl' D_{14,34} - \frac{1}{2} dx'_4 dl' D_{34,34}, \quad (17)$$

$$d\sigma_C \Lambda_{34}^{(C)} = -\frac{\sqrt{3}}{2} dx'_4 dl' D_{14,34} - \frac{1}{2} dx'_4 dl' D_{34,34}. \quad (18)$$

Here dl' denotes integration from $l' = 0$ to $l' = R$, R is quark separation from the string junction; dx'_4 denotes integration from $x'_4 = -T/2$ to $x'_4 = T/2$.

Using (5) the correlators entering (13-18) can be expressed through D, D_1 as

$$D_{14,14}(z) = D(z) + D_1(z) + (z_1^2 + z_4^2) \frac{dD_1}{dz^2}, \quad (19)$$

$$D_{34,34}(z) = D(z) + D_1(z) + (z_3^2 + z_4^2) \frac{dD_1}{dz^2}, \quad (20)$$

$$D_{14,34}(z) = D_{34,14}(z) = z_1 z_3 \frac{dD_1}{dz^2}. \quad (21)$$

From the symmetry of Fig.5 it is clear, that the resulting field distribution is symmetric under rotation in the (x_3, x_1) plane over angle $\frac{2\pi n}{3}$, $n = 0, 1, 2, \dots$, and indeed from (11-21) one can conclude that color electric field has this symmetry.

We have calculated the $\mathbf{E}^2(\mathbf{r}^2) = (E_1^{(3Q)})^2 + (E_3^{(3Q)})^2$ distribution, where $\mathbf{r} = (x_1, x_3)$, displayed on Fig.6 (a-c) for $R = T_g, 5T_g$ and $15T_g$ respectively. One can easily see the symmetry discussed above, and in addition a remarkable feature, - a hole in $\mathbf{E}^2(\mathbf{r}^2)$ near $\mathbf{r} = 0$. The hole profile, i.e. distribution of \mathbf{E}^2 along the x_3 axis, is depicted in Fig.6 (d) for given quark separations. As one can see, the hole shape does not depend on the quark separation. At separation $15T_g$ the string acquires its saturation value $E^{sat} = 1.8\text{GeV/fm}$. The radius of hole, i.e. distance from string junction at which \mathbf{E}^2 is half of its saturation value, is $1.75T_g$.

The physical origin of this hole is understandable: the fields \mathbf{E} are directed in three sheets $\Sigma_A, \Sigma_B, \Sigma_C$ and are perpendicular to the string-junction line; hence there is no preferred direction for the field \mathbf{E} at $\mathbf{r} = 0$. To get more quantitative insight into the problem, let us consider the line $x_1 = 0$ in the plane (x_1, x_3) and compute $E_1^{(3Q)}$ and $E_3^{(3Q)}$ as functions of x_3 . From (11), (12) one immediately obtains

$$E_1^{(3Q)}(x_1 = 0, x_3) = 0, \quad (22)$$

$$E_3^{(3Q)}(x_1 = 0, x_3) = \int_{-\frac{T}{2}}^{\frac{T}{2}} dx'_4 \int_0^R dl' \{ \tilde{D}(\sqrt{(x'_4)^2 + (x_3 - l')^2}) - \tilde{D}(\sqrt{(x'_4)^2 + \frac{3}{4}l'^2 + (x_3 + \frac{1}{2}l')^2}) \}, \quad (23)$$

where $\tilde{D} \equiv D_{34,34}(h)$. From (23) one can deduce that E_3 vanishes linearly at $x_3 = 0$ and grows fast for positive x_3 attaining a constant limit for $x_3 \sim \frac{1}{\mu}$ when $R\mu \gg 1$. Thus $\mathbf{E} = 0$ at the center of the hole and the radius of the hole is of the order of $r \sim \frac{1}{\mu} = T_g$.

4. We now go over to another topic, closely connected with the previous one, namely the static potential for QQQ system calculation. Choosing the same Y - shaped equilateral configuration one has from the cluster expansion of the Wilson loop $W^{(3Q)}$,

$$V^{(3Q)}(R) = -\lim_{T \rightarrow \infty} \frac{1}{T} \ln \langle W^{(3Q)}(R, T) \rangle = \\ = \sum_{a,b=A,B,C} \frac{1}{2} \int \int d\sigma_a(x) d\sigma_b(y) D_{a,b}(x, y) = \frac{1}{2} \sum_{a,b} V_{a,b}(R), \quad (24)$$

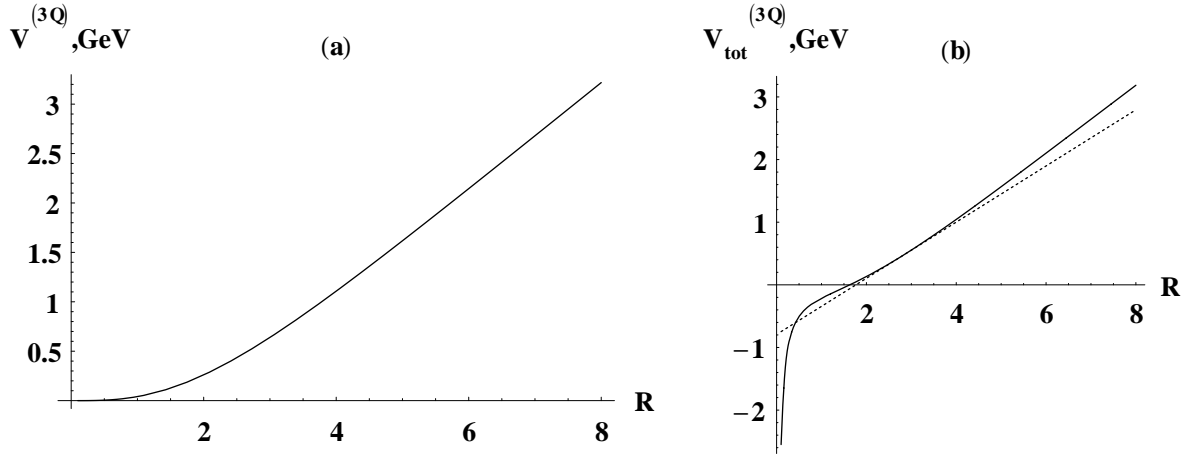


Figure 7: (a). The $3Q$ potential for the string junction configuration of Fig.5 as a function of distance from quark to string junction (in units of T_g). (b). The same as in (a) with perturbative one-gluon-exchange potential added.

where, e.g.

$$V_{A,A}(R) = \frac{1}{T} \int_{-\frac{T}{2}}^{\frac{T}{2}} dt \int_{-\frac{T}{2}}^{\frac{T}{2}} dt' \int_0^R dz \int_0^R dz' [D(h) + D_1 + h^2 \frac{dD_1}{dh^2}] \quad (25)$$

and $h^2 = (z - z')^2 + (t - t')^2$.

Using (13)-(18) one can easily find the nondiagonal terms, e.g.

$$V_{A,B}(R) = \frac{1}{T} \int_{-\frac{T}{2}}^{\frac{T}{2}} dt \int_{-\frac{T}{2}}^{\frac{T}{2}} dt' \int_0^R dl \int_0^R dl' [\frac{\sqrt{3}}{2} D_{14,34}(\tilde{h}) - \frac{1}{2} D_{34,34}(\tilde{h})], \quad (26)$$

where $\tilde{h}^2 = (t - t')^2 + \tilde{h}_1^2 + \tilde{h}_3^2$, $\tilde{h}_1 = -\frac{\sqrt{3}}{2} l'$, $\tilde{h}_3 = l + \frac{1}{2} l'$; and

$$D_{14,34}(\tilde{h}) = \tilde{h}_1 \tilde{h}_3 \frac{dD_1(\tilde{h}^2)}{d\tilde{h}^2}. \quad (27)$$

For $V_{A,C}(R)$ both (26) and (27) are valid, but the sign of \tilde{h}_1 is opposite to that of (27).

From symmetry of the problem it is clear that the whole potential is expressed through $V_{A,A}$, $V_{A,B}$, $V_{A,C}$ as

$$V^{(3Q)}(R) = \frac{3}{2} (V_{A,A} + V_{A,B} + V_{A,C}). \quad (28)$$

We plot this potential in Fig.7 together with the total potential including the perturbative one-gluon-exchange parts,

$$V_{tot}^{(3Q)}(R) = V^{(3Q)}(R) - \frac{2\alpha_s}{\sqrt{3}R}, \quad (29)$$

where $\alpha_s = 3/4e$; $e = 0.295$ from fit of the $Q\bar{Q}$ lattice potential by Cornell potential (see [13] and references therein). One can notice on Fig.7 that large-distance asymptotic of the $V^{(3Q)}(R)$ is equal to $3\sigma R$, as it should be. At $R = 3.5T_g$ the slope of $V^{(3Q)}$ is 2.6σ that is in accordance with recent lattice measurements of $V_{tot}^{(3Q)}(R)$ ([13]) which in the measured region $0.055 \leq R \leq 0.71$ fm were fitted by the Cornell potential with string tension 2.6σ .

5. We have calculated connected-probe field distributions for $Q\bar{Q}$ and QQQ cases using the lowest (Gaussian) field correlator. Since distribution of fields is the same as in lattice calculations of static potentials in [10], where the Gaussian correlator contributes 99% of the total result, one expects that higher correlators would not change our picture significantly.

The connected-probe analysis is essential for establishing direction of fields in the string and distinguishing color-electric and color-magnetic contributions, since due to properties of the Gaussian correlator (5) and relative weakness of D_1 term, the orientation of the probing plaquette $P_{\mu\nu}$ allows to fix the vector of the field in the string.

Our results for the $Q\bar{Q}$ case are in agreement with earlier calculations in [1, 2]. The bulk of the string fields is also in accordance with disconnected-probe analyses [3, 4].

The QQQ results are new and striking. A deep hole in the electric field distribution appears around the string-junction position, where electric field vanishes because of rigorous symmetry arguments. The hole has a radius of $1.75T_g$ and strongly suppresses fields in the middle of the heavy baryon. Since the Wilson loop for the QQQ configuration used to generate interaction is also applicable for light quarks [14], physical consequences of this hole can be in principle observable both for light and heavy hadrons. One consequence can be read off on Fig.7, where the nonperturbative part of the potential grows very slowly at small R , so that the asymptotic slope is obtained only at very large distances. Therefore an effective slope for ground-state hadrons can be some 10-20% smaller, the fact which is in agreement with relativistic quark model of baryons [15] and with recent lattice calculations of static QQQ potential [13].

One should note that the vanishing of fields at the string junction holds for directed field distribution, measured in the connected-probe analysis, and may not be true for field fluctuations, measured in the disconnected probe. This topic and other possible consequences of the hole in the middle of the baryon call for further investigations.

Financial support of the grants 00-02-17836 and 00-15-96786 is gratefully acknowledged.

The authors are grateful to N.O.Agasyan, A.B.Kaidalov, Yu.S.Kalashnikova, V.I.Shevchenko for useful remarks. D.K. is grateful to D.V.Chekin for discussion of software details.

References

- [1] A.Di Giacomo, M.Maggiore and S.Olejnik, Phys.Lett. **B236** (1990) 199; Nucl.Phys. **B347** (1990) 441
- [2] L.Del Debbio, A.Di Giacomo and Yu.A.Simonov, Phys.Lett. **B332** (1994) 111
- [3] Ch.Schlichter, G.S.Bali, K.Schilling, hep-lat/9412018
- [4] R.W.Haymaker, V.Singh, Y.Peng and J.Wosiek, Phys.Rev. **D53** (1996) 389
- [5] Ch.Schlichter, G.S.Bali, K.Schilling, Nucl.Phys.Proc.Suppl. **63** (1998) 519; *ibid* **42** (1995) 273; Phys.Rev. **D51** (1995) 5165
- [6] M.Rueter and H.G.Dosch, Z.Phys. **C66** (1995) 245
- [7] H.G.Dosch, O.Nachtmann and M.Rueter, hep-ph/9503386

- [8] H.G.Dosch, Phys.Lett. **B190** (1987) 177;
 H.G.Dosch and Yu.A.Simonov, Phys.Lett. **B205** (1988) 339;
 Yu.A.Simonov, Nucl.Phys. **B307** (1988) 512
- [9] Yu.A.Simonov, Phys.Usp. **39** 313 (1996)
- [10] G.S.Bali, hep-lat/9908021
- [11] Yu.A.Simonov, JETP Lett. **71** (2000) 187, hep-ph/0001244;
 V.I.Shevchenko and Yu.A.Simonov, hep-ph/0001299
- [12] M.Campostrini, A.Di Giacomo and G.Mussardo, Z.Phys. **C25** (1984) 173;
 A.Di Giacomo and H.Panagopoulos, Phys.Lett. **B285** (1992) 133;
 A.Di Giacomo, E.Meggiolaro and H.Panagopoulos, Nucl.Phys. **B483** (1997) 371
- [13] G.S.Bali, hep-ph/0001312
- [14] Yu.A.Simonov, Phys.Lett. **B228** (1989) 413;
 M.Fabre de la Ripelle and Yu.A.Simonov, Ann.Phys. (NY) **212** (1991) 235;
 B.O.Kerbikov and Yu.A.Simonov, Phys.Rev. D (in press) hep-ph/0001243
- [15] S.Capstick and N.Isgur, Phys.Rev. **D34** (1986) 2809

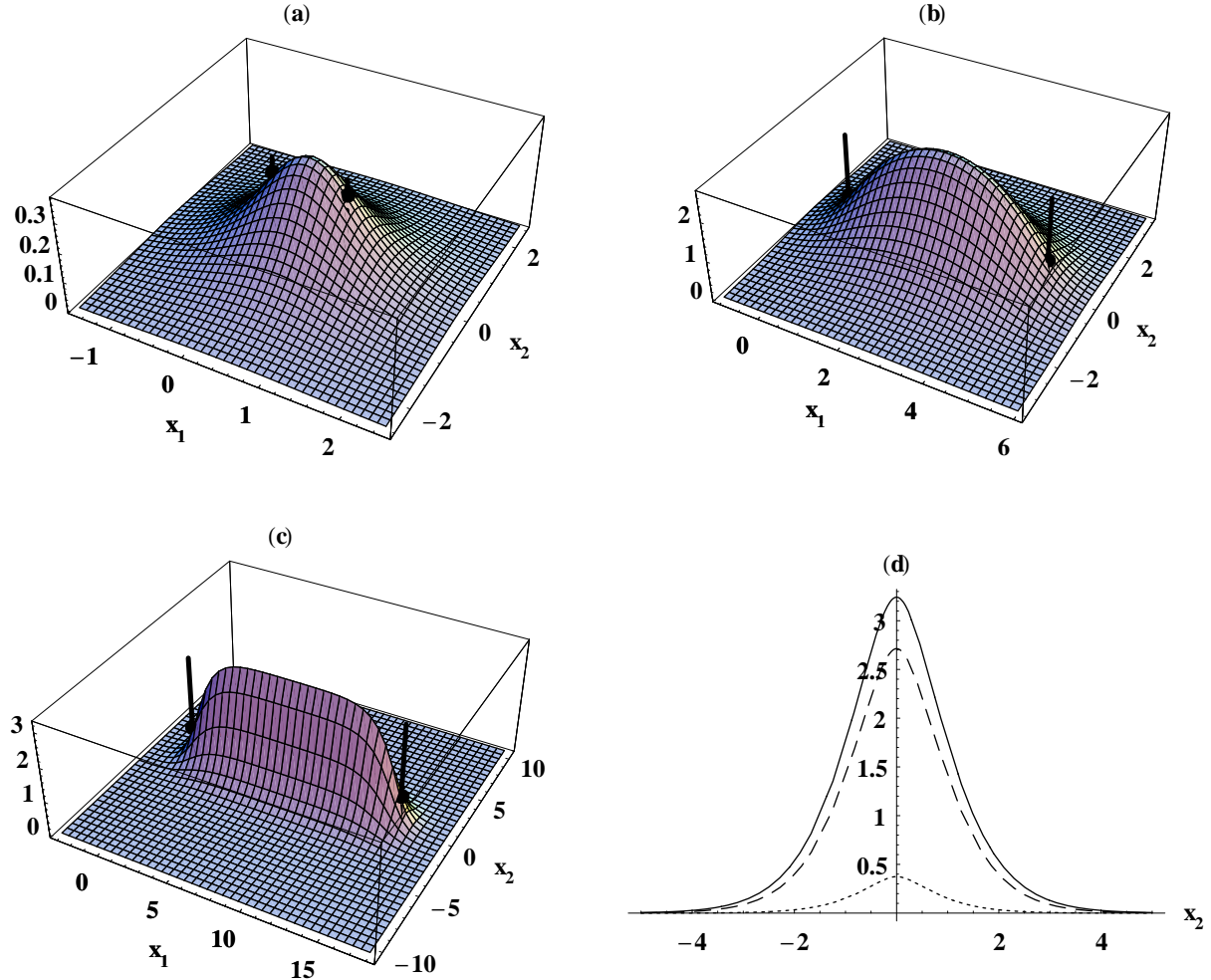


Figure 2: Distribution of the field E_1^2 measured in GeV^2/fm^2 around static $Q\bar{Q}$ sources as function of x_1 (distance along the string) and x_2 (distance from the string axis). Both distances are measured in units of T_g . Positions of Q and \bar{Q} are marked with points with vertical lines. The cases (a),(b),(c) refer to the interquark distances $R_{Q\bar{Q}} = 1, 5$ and $15T_g$. In Fig.2(d) the string profile (i.e. $E_1^2(x_2)$ distribution at the middle of the string) is shown, dotted, dashed and solid lines for the three interquark distances of Figs. 2(a), (b) and (c) respectively. Note the saturation of the string height and width at around $R \approx 5T_g$.

This figure "page10.png" is available in "png" format from:

<http://arxiv.org/ps/hep-ph/0006192v1>

This figure "page11.png" is available in "png" format from:

<http://arxiv.org/ps/hep-ph/0006192v1>